2. Literature Review

2.1. General

This chapter shows the comprehensive literature review studied for the individual objective. The chapter is divided into six sections, each section contains the literature reviewed for the specific objective.

2.2. Literature review:

1. **Objective:** To demonstrate a comparative assessment of discrepancy in the hydrological behaviour of the DEMs in terms of terrain representation at the catchment scale.

   The study of Sharma & Tiwari, (2014) shows noteworthy contrasts in hydrological properties of the two contemplated DEMs considering vertical accuracy assessment, hydrological simulation, empirical USLE model, and physical SWAT model. ArcSWAT simulation results uncover runoff predictions that are less sensitive to the selection of the DEMs. To delineate the drainage network that causes a significant effect on hydrological or hydraulic modeling and the comprehension of fluvial processes, Persendt & Gomez, (2016) selected different progressive flow accumulation threshold values. Ficklin et al., (2015) concluded that the DEM source and DEM resampling techniques (nearest neighbor, bilinear interpolation, cubic convolution, and majority) are less sensitive parameters as compared to DEM resolution in the SWAT model. Guth, (2010) compared the GDEM with SRTM 3 arcsecond data and computed the elevation, slope distributions, and geomorphometric parameters. Furthermore, they determined that the ASTER GDEM is essentially equivalent to SRTM 3 arcsecond data. In addition, they also reported that GDEM contains data anomalies or inconsistencies that corrupt its utilization for most applications. However, many studies have demonstrated that the outputs of hydrological models are influenced by DEM resolution (Chaplot, (2014); Wolock & Price, (1994)), DEM source and DEM resampling (Wang et al., (2012)).

   DEMs, however, contain local ‘‘pits’’ or ‘‘sinks’’ due to data errors in observation density, spatial sampling, interpolation process, data entry, or observer bias (Martz & Garbrecht, (1998); Martz & Garbrecht, (1999); Campbell, (1990)). As all surrounding cells are higher than a local sink cell, such local pits can cause biased extraction of flow directions and stream networks from DEMs. Therefore, there will be no outflow from the sink, resulting in internal drainage or storage (Nikolakopoulos et al., (2006); Winter & LaBaugh, (2006)).

   The evaluation of lower resolution data such as the Shuttle Radar Topography Mission (SRTM) and Advanced Thermal Emission and Reflection Radiometer (ASTER) was carried out by Jarihani et al., (2015) using the hydrodynamic models by (i) assessing the point accuracy and geometric co-registration error of the original DEMs; (ii) quantifying the effects of DEM preparation

methods (vegetation smoothed and hydrologically corrected) on hydrodynamic modeling relative accuracy; and (iii) quantifying the effect of the grid size (30–2000 m) of the digital elevation hydrodynamic model and the associated relative computational costs (run time) on relative accuracy in model outputs. The study highlights the important impact of the quality of the underlying DEM and, in particular, how sensitive hydrodynamic models are to preparation methods and how important vegetation smoothing and hydrological correction of the base topographic data are for modeling floods in low gradient and multichannel environments.

In order to improve the accuracy of the estimated topography, Pham et al., (2018) developed an approach by combining two complementary DEMs (ASTER GDEM 1 arcsecond and SRTM DEM 1 arcsecond) in regions of missing reference data. Moreover, the combination approach was based on formulating relationships between slopes and weights in sites with reference data. Then, to determine the combined weight of each DEM without using reference data, the developed relationships were applied to sites with similar geomorphology. When compared with the SRTM and ASTER GDEM products, the results indicate that combined DEMs offer significant improvements of 47% and 20% in mean bias over a mountainous site, and 16% and 58% at a low-relief site, respectively. DEM-derived drainages were also found to be more accurate for the combined DEMs as compared to the near-global DEMs in areas where reference data are not available. Furthermore, more accurate river networks can be derived by using higher resolution DEMs, but the best results may not be necessarily offered by the highest resolution data (Li & Wong, (2010)).

2. **Objective:** To develop an approach to analyze Sentinel–2 satellite data using traditional and principal component analysis based approaches to create land use and land cover map, which is a prerequisite for developing the curve number.

   PCA is a statistical procedure that transforms the input bands (with correlated variables) orthogonally from an input multivariate attribute space to a new multivariate attribute space (having linearly uncorrelated variables) whose axes are rotated with respect to each other. Transformation or dimensionality reduction of the data in the analysis compresses data by eliminating noise, redundancy, and irrelevant information. The linearly uncorrelated variables in new multivariate attribute space are called principal components. The first principal component (PC1 derived from the first eigenvector) is the direction in space along which projections have the largest variance. The subsequent principal component (PC2) is the direction which maximizes variance among all directions orthogonal to the previous principal component. The variances of the remaining principal component images decrease in order, as

denoted by the magnitudes of the corresponding eigen values (Li & Yeh, (1998); Deng et al., (2008)).

Recent studies have investigated PCA-based methods for cloud extraction scheme for multi-spectral images (Wu and Han, (2019)). Researchers have tried to manage imperfections in multivariate sensed data by using various PCA-based approaches. A PCA–OLS model was used by Firozjaei et al., (2019) for assessing the impact of surface biophysical parameters on land surface temperature variations. Massetti and Gil, (2020), and Abdu, (2019) employed PCA for classification accuracy and trend assessments of land cover- land use changes. Chen, (2020) used PCA of Sentinel-2 to map the mangrove of Dongzhaigang, China.

Empirical studies by researchers from diverse disciplines proved that land use and land cover information is key to various applications such as hydrology, agriculture, forest, environment, geology, and ecology (Weng, (2001); Hassan et al., (2016)). Decades of scientific research have shown considerable progress towards assessing land use and land cover (Turner et al., (2005)). Numerous effective methods and advanced classifiers have been applied to improve the performance of land use and land cover classification that is based on moderate resolution data. Researchers have used various methods to incorporate Landsat data into land-use change analyses (Ozesmi & Bauer, (2002); Lu et al., (2004); Rundquist et al., (2009); Zhang et al., (2000)).The complexity of the landscape, the selected remote sensing data, image processing, and classification methods, make it difficult to obtain reliable and accurate land use and land cover information (Manandhar et al, (2009)). Researchers have tried to overcome this problem from many different perspectives, with the purpose of seeking an efficient method for mapping LULC patterns. These studies range from conventional statistical approaches to more powerful machine learning algorithms that have enhanced the quality of the solutions for this problem. Traditional remote sensing data classification methods include maximum-likelihood classifier, distance measure, clustering or logistic regression. Over the last decade, more advanced methods such as decision trees, k-nearest-neighbors, random forest, neural networks and support vector machines have been used for LULC mapping (Yu et al., (2014); Cheng et al., (2015); Han et al., (2015)). Recently, a study on the state of the art of supervised methods for land use and land cover classification was performed by Khatami et al., (2016). It was reported that Support Vector Machine, k-nearest-neighbors, and Random Forest Tree generally provide better performance than other traditional classifiers, SVM being the most efficient method.

Support Vector Machine and Random Forest Tree classifiers are recent developments in the computational aspects of image classification. Their ability to minimize classification errors make them superior to the parametric classifiers such as Maximum likelihood estimation

classifier (Huang et al., (2002); Foody & Mathur, (2004); Pal et al., (2005)). SVM operate on principle of statistical learning theory principle, called structural risk minimization, which minimizes an upper bound on the generalization error. It aims at reaching the minimum of the upper bound on the error probability of the classifier by achieving a trade-off between the training set and the capacity. The basic approach in support vector machines is to identify a hyper-plane that produces optimal separation between the two classes. SVM classification with a hyper plane that maximizes the separating margin between the two classes is shown in Figure 2.1. The algorithm defines the multidimensional space in such a way that the gap between class clusters is as large as possible. The hyper-plane is developed using a subset of the data called the training data set and the generalizing ability of the developed hyper-plane is validated using an independent subset called testing data set. If the training dataset is not linearly separable, a kernel method is used to simulate a non-linear projection of the data in a higher dimensional space, where the classes are linearly separable (Oommen et al., (2008); Candade and Dixon, (2004)).

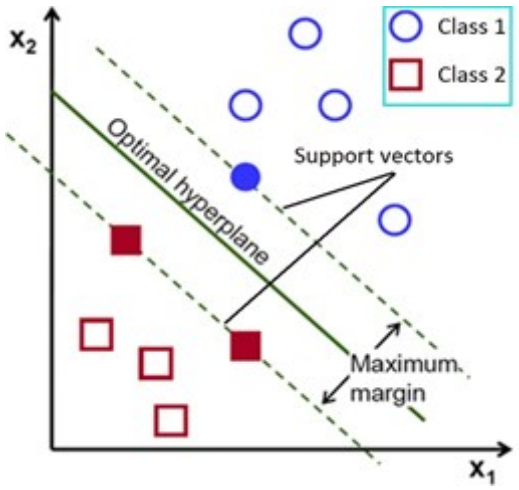

Figure 2.1: SVM classification with a hyper plane that maximizes the separating margin between the two classes.

Random Forest Tree is an ensemble bagging algorithm which is fast, easy to parameterize, and robust and has been frequently used for land use and land cover classification (Belgiu & Csillik, (2018); Immitzer et al., (2012); Ok et al., (2012); Scanlon et al., (2006); Pelletier, Valero et al., (2016)). Random Forest is a general term for ensemble methods using tree-type classifiers,$\{h(\boldsymbol{x}, \Theta_k)$, k=1, …,}, where **x** is the input vector and $\boldsymbol{\Theta}_k$are the independent and identically distributed random vectors (Breiman, (2001); Gislason et al., (2006); Rodriguez et al., (2012)). Hence, some data may be used more than once in the training of classifiers, while others might never be used. Thus, greater classifier stability is achieved, as it makes it more robust when facing slight variations in input data and, at the same time, it increases classification

accuracy. The trees are created by drawing a subset of training samples through replacement (a bagging approach). The random forest classifier consists of N trees, where N is the number of trees to be grown, which can be any value defined by the user. To classify a new dataset, each case of the datasets is passed down to each of the N trees. The forest chooses a class having the most out of N votes, for that case. Furthermore, when the RF makes a tree grow, it uses the best split of a random subset of input features or predictive variables in the division of every node, instead of using the best split variables. Therefore, this can decrease the strength of every single tree, but it reduces the correlation between the trees, which reduces the generalization error. The generalization error converges as the number of trees increases, therefore, the RF does not over fit the data. The output of the classifier is determined by a majority vote of the trees.

Use of machine-learning classification methods for land use and land cover extraction has become a major focus of the remote-sensing literature (Ghimire et al., (2012)). Machine-learning algorithms are generally able to model complex class signatures, can accept a variety of input training data, and do not make assumptions about the data distribution (i.e. nonparametric). A wide range of studies have generally found that these methods tend to produce higher accuracy compared to traditional parametric classifiers, especially for complex data with a high-dimensional feature space, i.e. many predictor variables (Pal and Mather, (2005); Ghimire et al., (2012)). Despite the increasing acceptance of machine-learning classifiers, parametric methods appear still to be commonly used in application and remain one of the major standards for benchmarking classification experiments.

3. **Objective:** To perform Morphometrical analysis of Vishwamitri watershed and prioritization of sub-watersheds for assessing the flood influencing characteristics of sub-watersheds of the Vishwamitri river.

   The quantitative study of the morphometric features of watersheds is of considerable importance in the prediction of flood behaviour. The watershed hydrological response can be connected to the physiographic features of the watershed (Altaf et al., (2012)). Morphometric watershed analysis offers important aspects of watershed characterization with a detailed description of the drainage scheme. Morphometric parameters such as watershed area, watershed perimeter, stream order, stream length, basin length, ruggedness number, form factor, circulatory ratio, compactness index, drainage density, drainage frequency, bifurcation ratio, drainage texture, relief ratio, and lemniscate ratio have been used to establish a primary hydrological diagnosis and to prioritize sub-watersheds according to their flood potential (Masoud, (2016); Bhat et al., (2019)). Ungauged watersheds with scarce information on soil, geology, geomorphology and hydrology, morphometric analysis are an excellent alternative to

understand the underlying factors that regulate hydrological behaviour (Altaf et al., (2013); Romshoo et al., (2013)). Traditional methods have generally been used for morphometric characterization of watersheds in the past (Magesh and Chandrasekar, (2014); Ozdemir and Bird, (2009)). However, the assessment of watershed morphometry has become more reliable, speedy, and economically productive with the advancement of geographic information systems, high-resolution Digital Elevation Models (DEMs), and remote sensing techniques (Ahmed et al., (2010)). Recently, Bhat et al., (2019) evaluated the flood influencing factors in the upper Jhelum basin, they delineated the upper Jhelum basin into ten sub-basins, followed by extraction of drainage network and morphometric parameters using ASTER DEM and topographic maps in Geographic Information System. The overall flood potential was determined on the basis of the compound values obtained for all morphometric parameters of each sub-basin. Lately, Sridhar and Ganapuram, (2021) used morphometric analysis and fuzzy analytical hierarchy process to prioritize the sub-watersheds of Peddavagu watershed of the Krishna river basin according to the degree of erosion. Several researches have successfully used morphometric parameters to estimate the flash food susceptibility of watersheds (Mahmood and Ur Rahman, (2019); Wani et al., (2018); Bisht et al., (2018); Prasad and Pani, (2017); Bannari et al., (2017)). After rainfall, water behaviour is determined by the morphometric characteristics of the basin. However, not only the morphometric properties but also the infiltration potential of rocks and soils, vegetative interception, the soil's preceding moisture state and land use properties of the surface of the watershed are used to assess the rainfall portion available for surface runoff. As a result, for ungauged watersheds or where data are not available, several researchers use runoff modeling in order to gain a comprehensive understanding of the hydrological response of the watershed (Karmokar and De, (2020)).

4. **Objective**: To identify potential runoff storage zones based on the various physical characteristics of the Vishwamitri watershed using a GIS-based conceptual framework that combines through analytic hierarchy process using multi criteria decision-making method.

   Water scarcity has become serious problem in several parts of the world, especially in developing nations like India (Kumar & Jhariya, (2017)). In India, ever increasing population exerts enormous pressure on the water resources of the country due to which per capita water availability is decreasing day by day (Singh et al., (2017)). There is a growing need for cost effective and time saving methods to identify areas that are suitable for water storage. Hence, it becomes necessary to tap the maximum possible water within the watershed. Before execution water storage structures require significant investment and hence it is important to identify the potential runoff storage zones for these structures. Remote sensing and Geographic

information systems (GIS) together fulfil this need by providing a conceptual framework for collecting and analysing spatial and non-spatial data (Krois and Schulte, (2014)). Proper selection of factors is of great importance for identifying sites for specific water storage structures. A review of the literature done by Ammar et al., (2016) found that a different number of layers have been used by researchers to rely on the availability of data for potential water storage areas or to identify sites suitable for rainwater harvesting. Promoting rain water harvesting in areas receiving less than 100 mm/year or more than 1000 mm/year of rains is not recommended (Kahinda et al., (2016); Mou et al., (1999); FAO, (2003); Mati et al., (2006)). In several studies related to the identification of water storage sites, the weighted linear combination technique has been used for the integration of biophysical layers in a GIS environment. Weerasinghe et al, (2011) focused on using a geographic information system (GIS) and remote sensing (RS) and developed a spatial analysis model named Geographic Water and Management Potential. The model was able to find potential water harvesting and storage sites for water storage and soil-moisture conservation on farms. In most studies, range of weights was decided arbitrarily or weights were assigned on the scale of 1–5 or 1–100, whereas only a few studies assigned weights on the standard 1–9 scale, as suggested by Saaty, (1987). De Winnaar et al., (2007) conducted a study in which the SCS-CN method was applied to identify potential runoff-harvesting sites in a small sub-catchment in South Africa. The input data included socio-economic data gathered from available data and from field surveys, a digital elevation model with 20-m resolution to extract slope information, a soil survey provided soil data, digital images and aerial photographs. Similarly, Ghani et al., (2013) explored potential rainwater storage sites by examining runoff patterns using a hydrologic model with the GIS / RS approach. A 90 meter digital elevation model was used as a source for catchment elevation data to determine flow direction, drainage lines and runoff. Number of researchers applied the Curve Number method to identify potential runoff-harvesting sites (e.g. De Winnaar et al., (2007); Jha et al., (2014)). Krois and Schulte, (2014) presented GIS and multi criteria evaluation approach to identify and rank sites for the implementation of soil and water conservation techniques within the Ronquillo watershed. Criteria maps were created by reclassifying the spatial maps based on the suitability level for each RWH technique. Pairwise comparison matrix method (analytic hierarchy process), calculated the relative-importance weight of each criterion for each rain water harvesting technique. The weighted overlay process in GIS determined the suitability maps for each rainwater harvesting technique. Rainfall, runoff coefficient, slope, land use, soil texture and soil depth were selected based on the FAO guidelines. The assessment of the dominance of one criterion over another was based on the authors' expertise and a literature survey.

A number of studies have been reported for site suitability using Multi Criteria Decision Making (MCDM) and Analytic Hierarchy Process (AHP) in GIS environment (Al-Adamat, (2008); Pauw et al., (2008); Kahinda et al., (2008); Mahmoud and Alazba, (2014)). AHP is a popular weighting method in the field of MCDM (Saaty, (1977); Rozos et al., (2011); Karimi and Zeinivand, (2019)). The AHP is a theory of measurement through a pairwise comparison matrix and relies on the judgments of experts to derive priority scales. It is used as higher cognitive process tool to determine the percentage importance of various criteria used in the determination of suitable sites. The AHP method consists of three main phases: construction of hierarchy, priority analysis of data and confirmation of consistency. According to the review study done by Ammar et al., (2016) on identification of suitable sites for water storage in arid and semi-arid regions, it was found out that the most common biophysical layers or criteria applied were slope followed by land use/land cover and soil type.

5. **Objective**: To develop an approach for operational flood extent mapping using Synthetic Aperture Radar (SAR) and preparation of flood inundation map for data scarce region using 2D flow modelling using rain on grid model.

SAR for flood hazard assessment:

Remote sensing promises exceptional capacity in catastrophe control owing to its regular acquisition function over a large spatial extent (Serpico et al. 2012; Nirupama & Simonovic (2007); Gitas et al., (2008); Khan, (2005)). Flooding is a complex phenomenon due to its heterogeneity and spectral diversity. The analysis of flood mapping require high spatial and temporal resolution images to track the rapidly retreating flood process (Zhang et al. 2014). Drastic variability in climate has accelerated the incidence of catastrophic flood events in the last decade (Chunming et al., (2005)). In any flood-related study, identification of the flood extent and susceptible areas is a prerequisite to assess the disaster impact. Flood mapping can best be achieved with the help of remote sensing due to the inaccessibility to the flood-affected regions. However, cloudy conditions reduce flood mapping accuracy below the acceptable levels in optical remote sensing.

Synthetic Aperture Radar (SAR) imaging is an efficient remote sensing technique offering well-developed, consistent, efficient, and reliable means of collecting information to extract earth's surface dielectric properties (Lee and Pottier, (2009)). The ability of SAR to penetrate clouds is extremely useful in flood-related studies. Synthetic aperture radar uses microwave radiation to illuminate the earth’s surface for recording the amplitude and phase of the back-scattered radiation, which makes the imaging process coherent. The active sensor of Sentinel-1 forms a SAR image by coherently processing the returning signals from successive radar pulses. Stronger or weaker final signals (output) are generated by the out-of-the-phase waves by constructively

or destructively interfering with each other. These interferences produce a seemingly random pattern of brighter and darker pixels giving the radar images a distinctly grainy appearance known as 'Speckle' (Goodman, (1976); Lee et al., (1994)). Speckle noise changes the spatial statistics of the underlying scene backscatter making the classification of imageries a difficult task (Durand et al., (1987)). To date, different classification algorithms, including the Support Vector Machine (SVM), Maximum Likelihood (ML), Classification and Regression Tree (CART), K-Nearest Neighbor (KNN), and Random Forest (RF), have been applied in various studies. The RF classifier is one of the most effective approaches for classification (Breiman, (2001)). Various studies have been conducted using pixel-based RF algorithm for wetland vegetation mapping using high spatial resolution SAR data (Amani et al., (2017); Fu et al., (2017); Mahdianpari et al., (2017)). Dumitru et al., (2015)) applied the SVM classifier for the rapid mapping of damage assessment for flood in Germany in 2013 and the tsunami in Japan in 2011 using TerraSAR-X pre- and post-flood data. A brief introduction of some well-known despeckling methods is presented below:

De-noising Methods

The presence of speckle is the major challenge in the SAR image processing. A speckle reduces the resolution of an image and the detectability of the ground targets. It also distorts the spatial patterns of surface characteristics and reduces the accuracy of image classification (Wang & Ge, (2012)). Speckles are signal-dependent and, therefore, act like multiplicative noise (Lee, (1981)).

I. Boxcar filter:

A simple averaging filter that replaces the center pixel in a 3×3 or a larger sized moving kernel with the mean value of kernel pixels. It has good performance in reducing speckles in a homogeneous area; however, it degrades spatial resolution due to indiscriminately averaging pixels from the inhomogeneous area and destroys the polarimetric properties (Lee & Pottier, (2009)). This easy operation can very well retain the polarimetric characteristics of certain pixels. However, it over filters the point targets, creates a combination of heterogeneous pixels and degrades the overall spatial information. The filter is simple and fast, however, it is not isotropic (i.e. circularly symmetric), but smooths further along diagonals than along rows and columns. Also, discontinuities are found in the smoothed image due to an abrupt cut-off of weights rather than decline gradually to null.

II. Gamma map filter:

This filter is based on the Bayesian analysis of image statistics. The scene reflectivity of the underlying image in Gamma-Map algorithm is assumed to be Gamma distributed rather than normally distributed, and speckle is noise within it. Thus this filter works best for geospatial

images containing homogenous areas such as oceans, forests, fields, etc. (Lopes et al., (2005)). It is given by following cubic equation (Frost et al., (1982).

$$\hat{I}^3 - \bar{I}\hat{I}^2 + \sigma(\hat{I} - DN)=0 \quad 2.1$$

$\hat{I}$ = *required value*

$\bar{I}$ = *local mean*

DN = *input value*

σ = *original image variance*

Gamma-Map approach has several advantages compared to the other filters, as it can simultaneously take into account realistic first and second order statistical models for both speckle and underlying scene reflectivity, and combine them through Bayesian inference. Thus this filter works best for geospatial images containing homogenous areas such as oceans, forests and fields.

III. *Frost filter:*

This filter uses local image statistics to remove high-frequency noise (speckles) while preserving features (edges) by averaging less in the edge areas. It replaces the pixel of interest with a weighted sum of the values within an n × n moving kernel (Qiu et al., (2004)). The despeckled pixel value is estimated using a sub-window of the processing window. The size of the sub-window varies as a function of the target local heterogeneity measured with a coefficient of variation.

$$\text{Digital number (DN)} = \sum_{nXn} k\alpha e^{-\alpha|t|} \quad 2.2$$

$\alpha = \left(\frac{4}{n\bar{\sigma}^2}\right)\left(\frac{\sigma^2}{\bar{I}^2}\right)$

k = *normalized constant*

$\bar{I}$ = *local mean*

σ = *local variance*

$\bar{\sigma}$ = *image coefficient of variation value*

$|t| = |X - X_0| + |Y - Y_0|$

n = *moving kernel size*

When uniform regions are filtered, the Frost filter acts as a mean filter. When high contrast regions are filtered, the filter acts as a high-pass filter with rapid decay of elements away from the filter centre. Thus, large uniform areas will tend to be smoothed out and speckle removed, whilst high contrast edges and other objects will retain their signal values and not be smoothed. After application of the Frost filter, the denoised images show better sharpness at the edges.

IV. *Lee filter:*

Lee filter is based on the assumption that the filtered or output pixel value is a weighted sum of the reference pixel value and the mean of the values within the kernel (Lee, (1981)). The filter removes the noise by minimizing either the mean square error or the weighted least square estimation (Qiu et al., (2004)). The Lee filter utilizes the statistical distribution of the digital number values within the moving kernel to estimate the value of the pixel of interest. This filter assumes the normal distribution for the noise in image data.

$$I_{out} = [mean] + K[U_{in} - mean] \quad (2.2)$$

I_{out} = *filtered output*

U_{in} = *unfiltered input*

mean = *average of pixels in a moving kernel*

$K = \frac{Var(x)}{mean^2\sigma^2 + Var(x)}$

Variance of × is defined as:

$$Var(x) = \frac{[variance\ within\ kernel] + [mean\ within\ kernel]^2}{\sigma^2 + 1} - [mean\ within\ kernel]^2$$

Lee's smoothing filter is adaptive to the local statistics in an image, however, it is an isotropic adaptive filter which cannot remove noise in the edge region effectively. Lee filter is reportedly superior in its ability to preserve prominent edges, linear features, point target, and texture information.

V. *Lee sigma filter:*

This filter is based on sigma probability of the Normal distribution. The sigma (Standard Deviation) of the entire scene is first computed and then each central pixel in a moving window is replaced with the average of only those neighborhood pixels that have intensities within a fixed sigma range of the center pixel. It is well known that, in the normal distribution, the two-sigma likelihood is 0.955. The pixels outside the two-sigma range are considered outliers and ignored.

$$Standard\ deviation\ of\ an\ image = \frac{\sqrt{variation}}{mean} = Coefficient\ of\ Variation = Sigma\ (\sigma) \quad (2.3)$$

Due to the use of a fixed sigma computed for the entire scene, (de et al., (2009)) found that the Lee sigma filter blurred some of the low-contrast edges and linear features.

VI. *Median filter:*

This filter is not an adaptive filter as it does not account for the particular speckle properties of the image. Destructive and constructive interferences in SAR information are represented by extreme values (low-value and high-value pixels), which are efficiently suppressed by the Median filter (Sheng & Xia, (1996); Qiu et al. (2004)).The median filter is successful at removing pulse and spike noise while retaining step and ramp functions. Therefore, the median filter is better than the mean filter in terms of preserving the edges between two different features,

but it does not preserve single pixel-wide features, which will be altered if speckle noise is present. Median filter preserves the texture information very well for small window size (3×3) but does not retain the mean value at an acceptable level. Since the median is less sensitive than the mean to extreme values (outliers), those extreme values are more effectively removed.

2D Hydraulic modelling for flood hazard assessment:

Flood inundation modelling plays an important role in obtaining knowledge on the spatial distribution of flood patterns (such as water depth and flow velocity) (Kim et al., (2014)). This will include details on the nature of the danger, any risks to public safety and possible financial losses. They may also be used to support emergency response actions and mitigation policies for future flood events (Asselman et al., (2009); Thakur et al., (2017)). They are also important for educating the public and decision makers and for receiving support for the development of appropriate governance. Several methods, like Soil Conservation Service (SCS) - Curve Number method, Cook's method and unit hydrograph method, have been developed by engineers to estimate the discharge for an ungauged watershed (Gioti et al., (2013); Wakode et al., (2013); Elkhrachy, (2015); Sudhakar et al., (2015); Abuzied et al., (2016); Iosub et al., (2020)). In recent years, the hydrodynamic modeling of flood events has been greatly enhanced due to the advancement of increasingly accurate computational tools, effective computing power and innovative topographic survey techniques. Generally, the fluid motion and fluid dynamics are defined by solving mathematical equations based on the principles of the conservation of mass and momentum (Fassoni-Andrade et al., (2018)). 2D models that solve full shallow water equations, although they are data-intensive and have a high computational demand, are stated to have the ability to simulate the timing and period of inundation with high accuracy (Dasallas et al., (2019); Costabile et al., (2015)). In flood control programs, simulation of the water levels, release, flood forecasting, and flood-prone areas are becoming more prominent. As a result, hydrological modeling has since become an important part of water resource management (Malik & Pal, (2020)), the latest HEC-RAS 5.0.7 is increasingly studied in the literature since this model is popular with water engineers dealing with flood risk problems. Recently Costabile et al., (2020) assessed the performance of HEC-RAS Version 5.0.7 for watershed scale 2-D hydrodynamic rainfall-runoff simulations and concluded that HEC-RAS can be considered in rainfall-runoff simulations as a reliable model for discharge hydrograph computation. Ongdas et al., (2020) showed the application of HEC-RAS for flood hazard maps generation for the Yesil (Ishim) river in Kazakhstan. They simulated different flood scenarios on the River Yesil (Ishim) and also compared different mesh sizes (25, 50 and 75 m), the obtained results indicated no significant difference in model performance. Quirogaa et al., (2016) highlighted the strong

performance of the flood scale simulated by HEC-RAS compared to the satellite picture of the Bolivian Amazon flood. The combined version 1-D/2-D of HEC-RAS demonstrated that, together with high accuracy of topographic data, observed events can be replicated in the water basin Vozinaki et al., (2017).

6. **Objective:** To quantify the effects of urban land forms on land surface temperature and modeling the spatial variation using machine learning. The models can help to predict land surface temperature under temporary cloud cover spots, which are present in the data at the time of the acquisition, using neighboring biophysical (cloud-free) independent variables relationship with land surface temperature.

   Large urbanized areas alter processes for energy and water balance and affect air movement dynamics. The increasing conversion of natural vegetation and agricultural land into urban (impervious) land, such as buildings, parking lots, roads, and other constructions. This has caused several environmental problems at local, regional and global levels, such as biophysical hazards (e.g., heat stress), decreases in agricultural land, decrease in green space, human thermal comfort, ecosystem balance and acute health challenges. Due to changes and complexity of the surface temperatures of urban land types, the thermal behavior of different urban compositions has been investigated. The complex and diverse spatial structure of the heat intensities also varies from city to city. Therefore, to develop relevant mitigation and response strategies, it is important to establish city-specific land temperature patterns.

   The land surface temperature is defined as the temperature felt when long-wave radiation and turbulent heat fluxes are exchanged within the surface-atmosphere interface (Tomlinson, (2011); Avdan & Jovanovska, (2016)). It has been used in several fields, including hydrological cycles, urban climate, climate change and evapotranspiration. Studies show that urban growth is increasing with associated vegetation loss, leading to urban microclimate alterations. In Baltimore City, USA, Zhao et al., (2016) were keen to build correlations between the land surface temperature and land use/land cover indices. In the study carried out in Tehran City of Iran, Haashemi et al., (2016) noted a seasonal variation in the land surface temperature and land use/land cover relationship. To understand the relationship between land surface temperature and land use/land cover, the investigation of the thermal signature of each land use/land cover form is important (Weng et al., (2004)). Spectral indices are the most widely used and applicable method in large-scale research to measure the urban surface characteristic. Evidence from the past studies shows the precise and significant results in urban surface characteristic computation using spectral indices (Min et al., (2018); Chen & Zhang, (2017); Handayani et al. (2018)). Different simulation techniques are available to model future land cover changes in an

area, as a result, future land surface temperature modeling of that area is equally possible. However, there is relatively limited work on the simulation of land surface temperature. Mallick et al., (2008) used linear regression for predicting surface temperature over land use/land cover classes using normalized difference vegetation index and fractional vegetation cover.

Two or more satellite images from different timescales were used to analyze land surface temperature patterns because cloud-free images were not available for a large number of studies. However, any resulting land surface temperature configuration can be affected by different environmental factors (wind speed, Sun's radiation, surface moisture, and humidity) by differing acquisition time conditions (Zhang et al., (2017); Ranagalage et al., (2018); Ranagalage et al, (2019)). Zeng et al., (2014) tried to reconstruct MODIS land surface temperature based on multitemporal classification and robust regression. Similarly, Shuai et al., (2014) used a spectral angle distance-weighting reconstruction method to fill pixels of the MODIS land surface temperature product. Ahmed et al., (2013) used multiple regression analysis considering (NDVI, NDBI, NDWI, and NDBal) as explanatory variables to predict land surface temperature. In a recent study, Shafizadeh-Moghadam et al., (2020) used machine learning models to simulate urban land surface temperature based on independent factors such as land use/land cover, solar radiation, altitude, appearance, distance to major roads, and Normalised Difference Vegetation Index (NDVI) models. Performance evaluation of the four models revealed a close performance in which their R^2 and Root Mean Square Error (RMSE) were between 60.6–62.1% and 2.56–2.60 °C, respectively.